Subject ID: R-005 Preference for oral or poster: oral

Simplified stability analysis of geosynthetic-reinforced embankment subjected to over-topping flow

Antoine DUTTINE[1] and Fumio TATSUOKA[2]

[1] Department of Engineering & Numerical Analysis, Integrated Geotechnology Institute Ltd, Tokyo, Japan
[2] Prof. Emeritus, University of Tokyo & Tokyo University of Science, Tokyo, Japan

ABSTRACT

Water-front or water-impounding embankments, such as river and coastal levees, tsunami barriers, fill dams etc. may collapse if the global stability of the downstream slope is lost by over-topping flow and/or seepage flow caused by flood and tsunami. To prevent the above, impervious slope protections, such as concrete panel facing or slab facing, are often employed. These slope protections become stable when connected to geosynthetic layers that reinforce the embankment body. Based on global safety factors evaluated by the modified Fellenius limit equilibrium circular slip stability analysis, the stability of an embankment downstream slope is analyzed. It is shown that the slope stability decreases with an increase in the depth of overtopping flow and/or the seepage force, whereas the stability increases effectively by the use of impervious slope protection connected to geosynthetic reinforcements.

Keywords: slope stability; over-topping flow; modified Fellenius slice method; seepage

1 INTRODUCTION

The downstream slopes of such embankments as river levees, coastal levees, tsunami barriers, fill dams, other types of reservoir etc. may collapse, often triggered by external or internal erosion and/or scouring, by deep over-topping flow and/or seepage caused by flood or tsunami, which may result in a total loss of cross-section (e.g., the Great East Japan Earthquake disaster, March 2011). To prevent the above, impervious slope protections, such as concrete panel facing and slab facing, are often arranged on the downstream slope. In addition, planar geosynthetic layers may be arranged which are reinforcing the embankment body and, being connected to the slope protection, stabilize the latter.

In this paper, effects of over-topping flow and seepage, as wells as the use of impervious slope protection and geosynthetic reinforcement, on the stability of embankment downstream slope are evaluated. To this end, equations for the global safety factors under various conditions were formulated based on the modified Fellenius limit equilibrium slice method. By performing a series of numerical analysis of a typical slope model, it is shown that the factor of safety decreases with an increase in the depth of over-topping flow and the seepage force, while it increases effectively by the use of impervious slope protection connected to geosynthetic layers reinforcing the embankment body. Analysis of external and internal erosion and scouring is beyond the scope of this study.

2 FORMULATION

To evaluate the individual or combined effects of the factors mentioned above, the six cases shown in Fig. 1 are analyzed. The equations relevant to these cases are formulated within the framework of the modified Fellenius method. In this method, it is assumed that, in each slice, the resultant of interslice effective earth pressures is always in parallel to the slice base (Fig. 2). The factor of safety F_s against circular slip (radius R) in terms of overall moment equilibrium is defined as:

$$\begin{cases} F_s = [F_{\text{global}}]_{\min} = [M_r / M_d]_{\min} \\ M_r = R \cdot \sum [S_{fi}] = R \cdot \sum [c'_i \cdot l_i + P'_i \cdot \tan\phi'_i] \\ M_d = R \cdot \sum [S_{wi}] = R \cdot \sum (W_i \cdot \sin\alpha_i) - M_w \end{cases} \tag{1}$$

where M_r is the resisting moment; M_d the driving moment; S_{fi} the soil shear strength (cohesion c'_i & friction angle Φ'_i) mobilized on the base of the ith slice (angle α_i & length l_i); S_{wi} the shear force acting on the slice base; P'_i the effective normal load on the slice base; W_i the total slice weight; and $-M_w$ the moment due to the overburden water pressure U_{AB} acting on the submerged part of the downstream slope (Fig. 2).

2.1 Case 1: Submerged slope without seepage and over-topping flow

In this case, Eq. 2 for Fs is obtained by substituting the following terms for P'_i and M_w into Eq. 1: $P'_i = (W_i - W_{bi})\cos\alpha_i = W'_i.\cos\alpha_i$; and $M_w = \Sigma W_{wi}\sin\alpha_i - U_{AD}.y_h/R$.

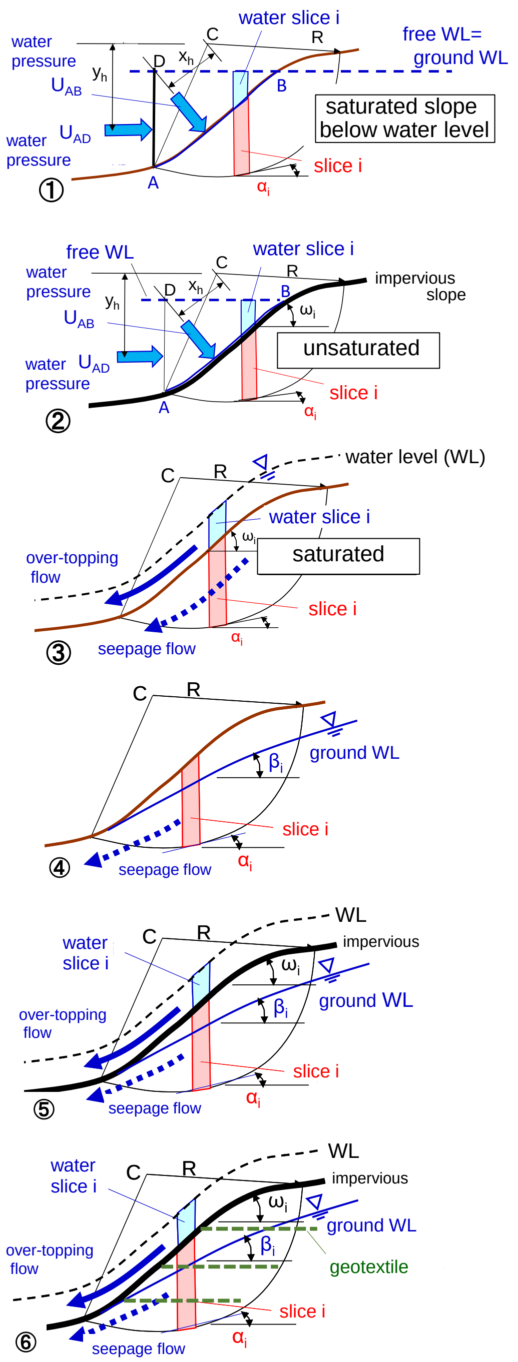

Case	Reservoir water	Impervious slope	Over-topping flow	Seepage flow	Geotextiles
①	✓				
②	✓	✓			
③			✓	✓	
④				✓	
⑤		✓	✓	✓	
⑥		✓	✓	✓	✓

Fig. 1. Six cases of downstream slope analyzed in this study.

This normal load P'_i is obtained by assuming that the resultant of interslice effective earth pressures is in parallel to the slice base and by the fact that the interstitial water pressure is acting horizontal on the vertical slice boundaries (i.e. the modified Fellenius method). W_{bi} is the buoyant force, W_{wi} the weight of the overburden water slice, U_{AD} the horizontal static water pressure resultant and y_h its vertical distance to the slip center (Fig. 1).

$$F_s=\frac{\sum[c'_i\cdot l_i+W'_i\cdot\cos\alpha_i\cdot\tan\phi'_i]}{\sum(W_i\cdot\sin\alpha_i)+\sum(W_{wi}\cdot\sin\alpha_i)-U_{AD}\cdot y_h/R} \tag{2}$$

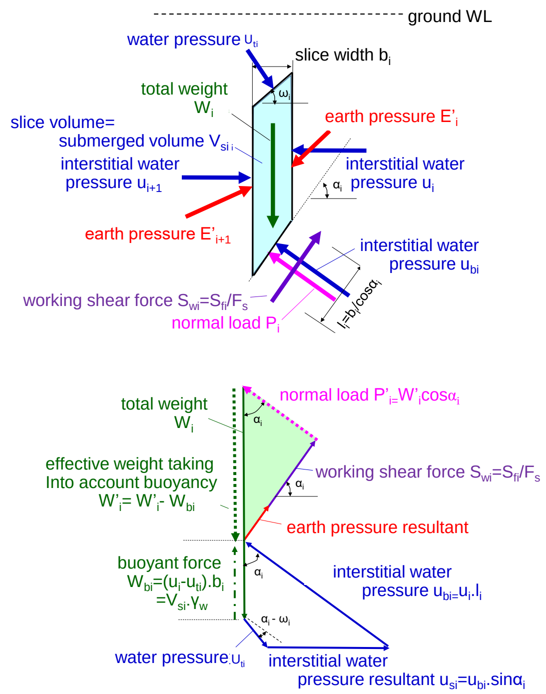

Fig. 2. Acting loads and forces polygon for a submerged slice without seepage and over-topping flow

2.2 Case 2: Slope with impervious slope protection and with static reservoir water

For an unsaturated slope covered by an impervious slope facing, F_s is given by Eq. 3, which is obtained by adding the beneficial effects of overburden water in the numerator of Eq. 2.

$$F_s=\frac{\sum[c'_i\cdot l_i+\{W_i\cdot\cos\alpha_i+\frac{W_{wi}}{\cos\omega_i}\cdot\cos(\alpha_i-\omega_i)\}\cdot\tan\phi'_i]}{\sum(W_i\cdot\sin\alpha_i)+\sum(W_{wi}\cdot\sin\alpha_i)-U_{AD}\cdot y_h/R} \tag{3}$$

where ω_i is the slice top angle and $W_{wi}/\cos\omega_i.\cos(\alpha_i-\omega_i)$ is the component of the overburden water pressure $W_{wi}/\cos\omega_i$ that is normal to the slice base. This component, combined with the term $W_i.\sin\alpha_i$ (where W_i is the total slice weight), greatly increases the slice normal load P'_i, thus the soil shear strength S_{fi}, thereby the F_s value, in comparison to case 1 (i.e., Eq. 2).

2.3 Case 3: Fully submerged slope subjected to over-topping flow & seepage

F_s is given by Eq. 4, for which, in comparison to Eq. 2, terms accounting for over-topping flow and seepage are added to the numerator while the component for horizontal static water pressure U_{AD} is removed from the denominator. Both of the above may largely decrease the F_s value.

$$F_s = \frac{\sum[c'_i \cdot l_i + [W_i \cdot \cos\alpha_i - W_{bi} \cdot \{\cos\alpha_i + \sin\omega_i \cdot \sin(\alpha_i - \omega_i)\}] \cdot \tan\phi'_i]}{\sum(W_i \cdot \sin\alpha_i) + \sum(W_{wi} \cdot \sin\alpha_i)} \quad (4)$$

ω_i is the seepage flow angle in slice i, which is the same as the angle α_i at the top of each slice. Taking $\alpha_i = \omega_i$, the formula of the numerator of Eq. 4 returns to the one of the numerator of Eq. 2 (for the case with no over-topping flow and no seepage flow), whereas the over-topping flow height should be accounted for when evaluating the water slice weight W_{wi} in Eq. 4

2.4 Case 4: Partially saturated slope subjected to seepage flow without over-topping flow

Eq. 5 is obtained by replacing ω_i in Eq. 4 with the seepage flow angle β_i which is basically different from the slice top angle ω_i and the slice base angle α_i.

$$F_s = \frac{\sum[c'_i \cdot l_i + [W_i \cdot \cos\alpha_i - W_{bi} \cdot \{\cos\alpha_i + \sin\beta_i \cdot \sin(\alpha_i - \beta_i)\}] \cdot \tan\phi'_i]}{\sum(W_i \cdot \sin\alpha_i)} \quad (5)$$

The effect of seepage flow in the term including $\sin(\alpha_i\text{-}\beta_i)$ may become either positive or negative depending on the sign of $\alpha_i\text{-}\beta_i$ in respective slices.

2.5 Case 5: Partially saturated slope with impervious slope protection subjected to over-topping flow & seepage

F_s is given by Eq. 6, for which effects of overtopping flow are added to the numerator and denominator of Eq. 5 via the water slice weight W_{wi}.

$$F_s = \frac{\sum[c'_i \cdot l_i + [W_i \cdot \cos\alpha_i - W_{bi} \cdot \{\cos\alpha_i + \sin\beta_i \cdot \sin(\alpha_i - \beta_i)\} + \theta_i \cdot W_{wi} \cdot \cos\alpha_i] \cdot \tan\phi'_i]}{\sum(W_i \cdot \sin\alpha_i) + \sum(W_{wi} \cdot \sin\alpha_i)} \quad (6)$$

θ_i represents the proportion of W_{wi} transmitted to the slice base increasing P'_i. It is assumed that θ_i is equal to the ratio of the volume of the unsaturated zone to the total slice volume, $\theta_i = A_D/(A_D + A_W)$. θ_i= 1.0 means that the slice is entirely unsaturated with W_{wi} fully increasing P'_i at the slice base, similar to case 2; while θ_i= 0 means that the slice is entirely saturated with W_{wi} not increasing P'_i, similar to cases 1 & 3.

2.6 Case 6: Slope in case 5 that is geosynthetic-reinforced

Effects of tensile forces in the reinforcement layers are simply added to the numerator of Eq. 6 (case 5).

$$\begin{cases} F_s = \dfrac{\sum[c'_i \cdot l_i + [W_i \cdot \cos\alpha_i - W_{bi}\{\cos\alpha_i + \sin\beta_i \sin(\alpha_i - \beta_i)\} + \theta_i \cdot W_{wi}\cos\alpha_i]\tan\phi'_i] + \sum T_{ri}}{\sum(W_i \cdot \sin\alpha_i) + \sum(W_{wi} \cdot \sin\alpha_i)} \\ T_{r\text{-}i} = T_i \cdot \sin\alpha_i + T_i \cdot \cos\alpha_i \cdot \tan\phi'_i \quad ; \quad T_i = \min\left\{T_{k\text{-}i}\ ;\ T_{p\text{-}i} = 2\int \sigma'_{v\text{-}i} \cdot \tan\phi' \cdot dx\right\} \end{cases} \quad (7)$$

T_{ri} is the resistance mobilized along the slice base (angle α_i) by the ith reinforcement layer having the allowable strength T_i. T_i is the minimum of the allowable tensile rupture strength $T_{k.i}$ and the allowable pull out strength $T_{p.i}$. For $T_{p.i}$, the soil/reinforcement interface friction angle is assumed to be equal to the soil internal friction angle Φ'; σ'_{vi} is the effective over burden pressure; and x is the reinforcement longitudinal axis (= 0 at the slip surface).

Further details on the derivation of Eqs. 2 to 7 are given in Tatsuoka & Duttine (2007a,b).

3 ANALYSIS OF MODEL SLOPE

Eqs. 2 to 7 were implemented in the stability analysis computer code developed by Duttine et al. (2018). The stability of a typical embankment slope (Fig. 3) was analyzed, in which the height is 15 m; the slope 1:2; and the soil unit weight & strength γ_t=19kN/m^3, γ_{sat}=20kN/m^3, c'=6kPa & Φ'=40^o. These values are typically used in the slope stability analysis following the Japanese railways design codes. In case 6, a typical reinforcement rupture tensile strength T_k= 30kN/m was used. The hydraulic conditions in cases 1 - 6 are depicted in Fig. 3.

Two sets of analysis were performed in cases 1 - 6 (Table 1). In the first set (A), to confirm the stability of the analysis, the safety factor was obtained for a fixed circular slip that is the critical circular slip, exhibiting the minimum F_s, in case 1 (Fig. 3). In the second set of analysis (B), the critical circular slip exhibiting the minimum F_s was obtained in each case (Fig. 4).

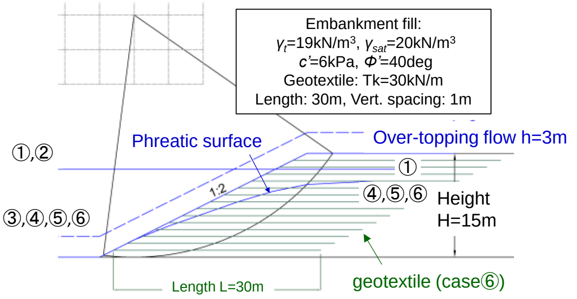

Fig. 3. Critical circular slip showing the minimum F_s in case 1, used in all the other cases (analysis set A):

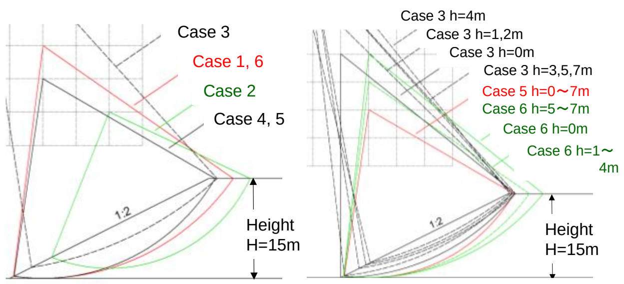

Fig. 4. (left) Critical circular slips showing the minimum F_s in each of cases 1 to 6 (h= 3 m); and (right) those for different over-topping depths h in cases 3, 5 & 6 (analysis set B):

Fig. 5 compares the F_s values obtained in cases 1 - 6 by analysis set A (Fig. 3) and set B (Fig. 4). It may be seen that the F_s value by set B is always smaller than the one by set A. By comparing the F_s values in cases 2 to 6 with the one in case 1 (a slope submerged with static water) and with each other, the effects of the influencing factors can be evaluated. Case 2: the impervious slope protection that makes the slope entirely unsaturated drastically increases the F_s value. Case 4: Internal seepage significantly decreases the F_s value. Case 3: the F_s value decreases by the overtopping flow, to a value less than unity in this case where a saturated slope does not have impervious slope protection. Case 5: compared with case 3, the F_s value noticeably increases by the presence of impervious slope protection that creates an unsaturated zone immediately below the slope surface protection. Case 6: compared with case 5, the F_s value further increases by the use of geosynthetic reinforcement.

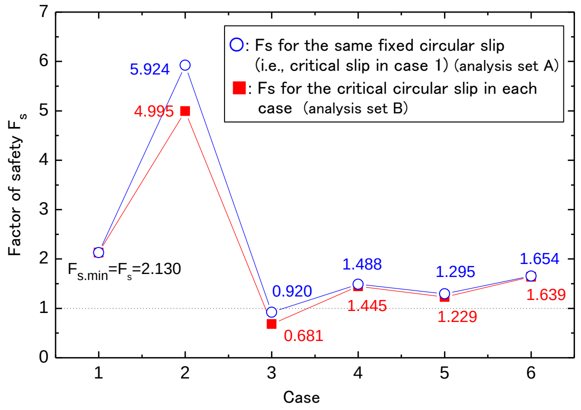

Fig. 5. Fs values for each case (for the model shown in Fig. 3)

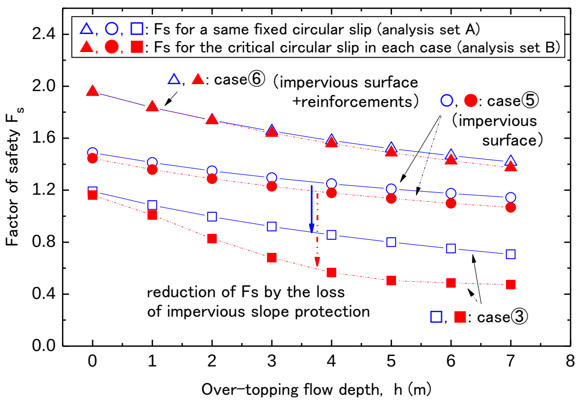

Fig. 6. Relation between F_s values and over-topping flow height

Fig. 6 shows the relationships between the F_s values obtained by analysis sets A and B and the overtopping flow height h in the cases 3, 5 and 6. In any of these cases, the F_s value consistently decreases with an increase in h. With the use of impervious slope protection (case 5), the F_s value is maintained larger than unity even when h reaches 7m. With the additional use of reinforcement (case 6), the F_s value when h=7m is as high as around 1.4. In contrast, in case 3 (without impervious slope protection), the F_s value drops quickly with an increase in h, with F_s (set B) becoming nearly unity already when h=1m. In case 5, the impervious slope protection may be easily lost, as it is not connected to reinforcement layers as in case 6. Thus, the F_s value may quickly drop to the value in case 3. Besides, in case 3, it is much more likely than in case 6 that external and/or internal erosion, and/or scouring, take place, resulting into a further decrease in the F_s value from those (set B) presented in Fig. 6.

When the computed value of F_s becomes less than unity, the static equilibrium is lost and the slip starts exhibiting residual shear displacements. In cases 3, 5 and 6, when the time history of over-topping flow depth $h(t)$ is provided, the residual slip displacements can be computed based on Eqs. 4, 6 and 7, similarly as in a Newmark sliding block seismic analysis.

4 CONCLUSIONS

To evaluate the effects of over-topping flow, internal seepage, as well as the use of impervious slope protection and geosynthetic reinforcements on the stability of an embankment downstream slope, a series of stability analysis was performed based on the safety factor equations formulated in the simple framework of the modified Fellenius slice stability analysis. A typical 15m-high embankment slope was analyzed. It was confirmed that the factor of safety decreases by the over-topping flow and internal seepage, whereas it increases by the use of impervious slope protection and further by the use of geosynthetic reinforcement layers connected to the slope protection. These results indicate that the combined use of impervious slope protection and geosynthetic reinforcement is very effective to protect the embankment slope against the over-topping flow and seepage flow.

REFERENCES

The Japanese Geotechnical Society (2011). GeoHazards during earthquakes and mitigation measures – Lessons and recommendations from the 2011 Great East Japan Earthquake, 84p., Japanese Geotechnical Society eds.

Design Standards for Railway Structures and Commentary (Earth Structures). (2007). Railway Bureau of the Ministry of Land, Infrastructures and Transport, Gov. of Japan and Railway Technical Research Institute eds., 27p.

Duttine, A., Tatsuoka, F., Shinbo, T. and Mohri, Y. (2018). A new simplified seismic stability analysis taking into account degradation of soil undrained stress – strain properties and effects of compaction, Proc. Int. Sym. on Qualification of dynamic analyses of dams and their equipment, Saint-Malo, France (eds. Fry, J.-J. & Matsumoto, N.), 215-234

Fellenius, W. (1936). Calculation of the stability of earth dams, Proc.2nd Congress on Large Dams, Washington, 445–462.

Tatsuoka, F. and Duttine, A. (2017a). Several remarks on the slope stability analysis by the ordinary slice method, Engineering for Dams, No.361, January, 5-30 (in Japanese)

Tatsuoka, F. and Duttine, A. (2017b). Several remarks on the limit equilibrium circular slope stability by the slice method, Proc. 52nd Japan National Conference on Geotechnical Engineering, Nagoya, 991-992 (in Japanese)